RSC Advances

ROYAL SOCIETY OF CHEMISTRY

www.rsc.org/advances

BF_3 bonded nano Fe_3O_4 (BF_3/MNPs): an efficient magnetically recyclable catalyst for the synthesis of 1,4-dihydropyrano[2,3-c]pyrazole derivatives

Mohammad Abdollahi-Alibeik*, Ali Moaddeli, Kianoosh Masoomi

[a]*Department of Chemistry, Yazd University, Yazd 89158-13149, Iran*

Abstract

Simple and efficient procedure for the synthesis of 1,4-dihydropyrano[2,3-c]pyrazole derivatives has been developed by one-pot three-component reaction of various aldehydes with malononitrile and 3-Methyl-1-phenyl-2-pyrazoline-5-one in the presence BF_3/MNPs as a novel nanostructured, heterogeneous and reusable catalyst. In this research, BF_3/MNPs nanoparticles were prepared at three calcination temperature and characterized by various techniques. The characterization and optimization results show that the catalyst with calcination temperature of 450 °C has the best catalytic activity. The nano-sized magnetite catalyst were recovered by simple separation with an external magnet and reused for several cycles without considerable loss of activity.

Keywords: magnetite nano particles; solid acid catalyst; magnetite recoverable catalyst; pyrane; multi-component reaction.

Introduction

Many conventional liquid inorganic acids, such as HNO_3, BF_3 and H_2SO_4 have been replaced by heterogeneous solid acid catalysts in acid-catalyzed organic transformations. Environmental pollution and difficulties in handling and separation of such homogeneous catalyst and also contamination of the products by residual catalyst, greatly restrict their applications from a process and economic point of view. Immobilization of inorganic acid on solid supports is a suitable way to improvement of mentioned drawbacks and this way

*Corresponding author
Mohammad Abdollahi-Alibeik, Department of Chemistry, Yazd University, Yazd 89158-13149, Iran Tel.: +98-35-31232659; fax: +98-35-38210644
E-mail address: abdollahi@yazd.ac.ir, moabdollaho@gmail.com

combine high surface area with the additional benefit of relatively facile recovery and regeneration.[1]

Solid-supported catalysts are an important and growing arena in heterogeneous catalysis. Therefore, a key challenge is to use a suitable and stable support with a large surface area to reach high accessibility to maximum active catalytic sites and maximum catalyst loading. Nano-sized solid-supports such as ZrO_2 [2, 3], TiO_2 [4, 5], Al_2O_3 [6], ZnO [7] and SiO_2 [8, 9] have attracted much attention due to their versatile physical surface and catalytic properties and applications in catalysis. However, conventional separation methods for these tiny support particles may become inefficient.

Magnetite nanoparticles are one of the most widely studied materials in multi-disciplinary research including biotechnology [10], biomedicine [11], magnetic resonance imaging (MRI) [12], targeted drug delivery [13] and catalysis [14, 15]. As the catalyst, magnetite has been used in several important commercial processes such as ammonia synthesis [16], water gas shift reaction [17] and Fischer-Tropsch reaction [18], which are important routes to get high value intermediates for chemical and petrochemical industries.

Recently, nano-magnetite has found versatile applications as a solid-support for preparation of recyclable catalysts in the development of sustainable methodologies [19]. Surface functionalization of magnetic nanoparticles is a well-designed way to bridge the gap between heterogeneous and homogeneous catalysis to increase catalytic activity of MNPs [20-22]. Due to its magnetic properties, it is also useful as component of several catalysts and adsorbents for different applications, allowing its separation from medium after reaction.

Fused pyran derivatives represent an important class of compounds which possess high activity profile due to their wide range of biological activities such as antimicrobial [23], antiviral [24] and cancer therapy [25]. Fused Pyrans to pyrazoles as pyranopyrazoles are an important class of heterocyclic compounds. They find applications as biodegradable agrochemicals [26] and pharmaceutical ingredients [27, 28]. The first synthetic method of this nucleus has been reported by Junek and co-workers by the reaction between 3-methyl-1-phenylpyrazolin- 5-one and tetracyanoethylene [29]. Afterward, various precursors and various acidic [30, 31] or basic [27, 32-34] catalysts has been introduced for the synthesis of pyranopyrazoles.

In this research, we supported BF_3 on Fe_3O_4 and bonded it to the support using thermal operations at various temperature as a novel solid acid and magnetically recoverable catalyst for the synthesis of pyranopyrazoles through multi-component reaction of 3-methyl-1-phenyl-1H-pyrazol-5(4H)-one, malononitrile and various aromatic aldehydes (Scheme 1).

Scheme 1.

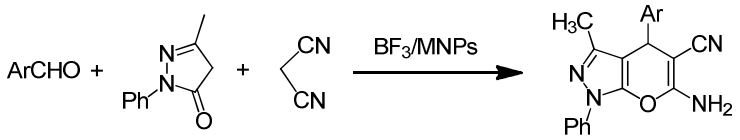

2. Experimental

2. 1. Materials and methods

All chemicals were commercial products. All reactions were monitored by (Thin Layer Chromatography) TLC and all yields refer to isolated products. ^{1}H and ^{13}C NMR spectra were recorded in DMSO-d_6 on a Bruker DRX-400 AVANCE (400 MHz for ^{1}H and 100 MHz for ^{13}C) spectrometer. Infrared spectra of the catalysts and reaction products were recorded on a Bruker FT-IR Equinox-55 spectrophotometer in KBr disks. XRD patterns were recorded on a Bruker D8 ADVANCE X-ray diffractometer using nickel filtered Cu Kα radiation (λ = 1.5406 Å). Scanning electron microscopy (SEM) was performed using KYKY-EM3200 instrument. Potentiometric data was collected using pH/mV meter, AZ model 86502-pH/ORP. ICP analysis was performed by VARIAN model Vista-pro instrument.

2. 2. Preparation of MNPs

Fe_3O_4-MN was prepared by co-precipitation method as reported [35]. In a typical procedure 0.5 M ferrous chloride (10 mL) and 0.5 M ferric chloride (10 mL) were mixed in a glass beaker. To this solution, 12 M NH_4OH (60 mL) was added drop by drop with continuous stirring. The resulting black precipitate was kept for 2 h. The precipitate was washed three times with deionized water (20 mL) to remove excess NH_3.

2. 3. Preparation of BF_3/MNPs

A mixture of MNPs (1 g), toluene (10 mL) and $BF_3{\cdot}Et_2O$ (3 mmol) was stirred for 2 h at room temperature. The suspension was separated by centrifuge and washed with toluene (10 mL). The solid was dried in an oven at 120 °C for 1 h and then calcined at 350, 400 or 450 °C for 2 h. The samples were labeled as BF_3/MNPs-X where X is the final calcination temperature.

Scheme 2. Preparation of the BF_3/MNPs catalyst

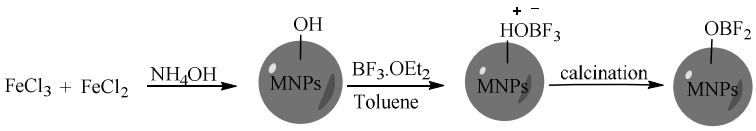

2. 4. General procedure for the synthesis of derivatives

A mixture of aryl aldehyde **1** (1 mmol), 3-Methyl-1-phenyl-2-pyrazoline-5-one (1 mmol) malononitrile **4** (1 mmol) and BF_3/MNPs (100 mg) was stirred in ethanol (5 mL) at 80 °C for mentioned times in Table 2. After completion of the reaction (monitored by TLC), the catalyst was separated from solid product by an external magnet, and product washed with small amounts of water (10 mL) and ethanol (5 mL) then recrystallized from ethanol to give the pure products **4a-j**.

2. 5. Physical and spectroscopic data for selected compounds

6-amino-3-methyl-4-(4-chlorophenyl)-1-phenyl-1,4-dihydropyrano[2,3-c]pyrazole-5-carbonitrile (4a):

^{1}H NMR (400 MHz, DMSO-d_6) : δ (ppm) = 7.79 (d, , J = 8 Hz, 2H), 7.50 (t, J = 8 Hz, 2H), 7.42 (d, , J = 8 Hz, 2H), 7.30-7.35 (m, 3H), 7.27 (s, NH_2), 4.74 (s, 1H), 1.80 (s, 3H); ^{13}C NMR (100 MHz, DMSO-d_6): δ (ppm) = 188.0, 159.3, 145.2, 143.6, 137.5, 129.3, 128.5, 127.8, 127.7, 127.0, 126.1, 119.9, 98.6, 58.1, 36.7, 12.5. FT-IR (KBr disk): 3448, 3323, 2198, 1660, 1519, 1490, 1392, 1128, 756 cm^{-1}.

6-amino-3-methyl-1,4-diphenyl-1,4-dihydropyrano[2,3-c]pyrazole-5-carbonitrile (4b)

^{1}H NMR (400 MHz, DMSO-d_6) : δ (ppm) = 7.79 (d, J = 8 Hz, 2H), 7.50 (t, J = 8 Hz, 2H), 7.33-7.38 (m, 3H), 7.25-7.29 (m, 3H), 7.23 (s, NH_2), 4.69 (s ,1H), 1.79 (s ,3H); ^{13}C NMR (100 MHz, DMSO-d_6): δ (ppm) = 181.0, 159.4, 145.2, 143.6, 137.5, 129.3, 128.5, 127.8, 127.0, 126.1, 119.9, 109.5, 98.6, 58.1, 36.7, 12.5. FT-IR (KBr disk): 733, 1027, 1065, 1125, 1264, 1385, 1444, 1515, 1592, 2198, 3324, 3471 cm^{-1}.

6-amino-3-methyl-4-(4-nitrophenyl)-1-phenyl-1,4-dihydropyrano[2,3-c]pyrazole-5-carbonitrile (4c)

^{1}H NMR (400 MHz, DMSO-d_6) : δ (ppm) = 8.24 (d, J = 8.8 Hz, 2H), 7.80 (d, J = 8.4 Hz, 2H), 7.59 (d, J = 8.8 Hz 2H), 7.51 (t, J = 7.6 Hz, 2H), 7.40 (s, NH_2), 7.34 (t, J = 6.4 , 1H), 4.94 (s ,1H), 1.80 (s ,3H); ^{13}C NMR (100 MHz, DMSO-d_6): δ (ppm) = 181.4, 159.6, 151.2,

146.6, 145.1, 137.4, 129.3, 129.2, 126.3, 123.9, 120.1, 97.6, 66.6, 36.3, 12.5. FT-IR (KBr disk): 3338, 3213, 2191, 1666, 1595, 1517, 1402, 1350, 1132, 821 cm^{-1}.

6-amino-3-methyl-4-(3-nitrophenyl)-1-phenyl-1,4-dihydropyrano[2,3-c]pyrazole-5-carbonitrile (4j)

^{1}H NMR (400 MHz, DMSO-d_6) : δ (ppm) = 8.16-8.17 (m, 2H), 7.79 (m, 3H), 7.68 (t, 1H, *J*=8Hz), 7.51 (t, 2H, *J*=8Hz), 7.38 (s, NH_2), 7.34 (t, 1H, *J*=8Hz), 4.98 (s, 1H), 1.81 (s, 3H)); ^{13}C NMR (100 MHz, DMSO-d_6): δ (ppm) = 159.7, 147.9, 145.9, 145.1, 144.0, 137.4, 134.7, 130.3, 129.3, 126.3, 122.2, 120.1, 119.7, 97.6, 57.0, 36.1, 12.6. FT-IR (KBr disk): 3437, 3298, 2194, 1651, 1595, 1517, 1400, 1352, 1263, 1122, 1070, 756, 694 cm^{-1}.

3. Results and discussions

3. 1. The catalyst characterization

Fig. 1 represents the results of scanning electron microscopy (SEM) in order to investigate the particle size and morphology of the catalysts. The SEM of the MNPs and BF_3/MNPs shows spherical nanoparticles with sizes of <100 nm. In the case of BF_3/MNPs, partial agglomeration is observed due to BF_3 treatment on MNPs surface and also calcination, but this treatment has not dramatically effect on the nanoparticle shapes. To investigate the elemental component of the BF_3/MNPs-450, EDX analysis was performed and shown in Fig. 3c. Presence of the Fe and O related to the MNPs is obvious. In addition, EDX analysis shows considerable content of the F. Moreover the loading level of boron on the surface of BF_3/MNPs-450 was estimated to be at about 0.5 mmol g^{-1} with an ICP method and the fluoride contents of BF_3/MNPs-450 was estimated to be at about 0.75 mmol g^{-1} and it was measured by a potentiometric method using a fluoride ion-selective electrode. These results verify presence of B-F species in the catalyst and the obtained B/F molar ratio of 3/2 shows that boron species on the MNPs surface. The B/F molar ratio of 3/2 suggests that a covalent bond between oxygen of Fe_3O_4 and boron is created due to evolution of HF during calcination.

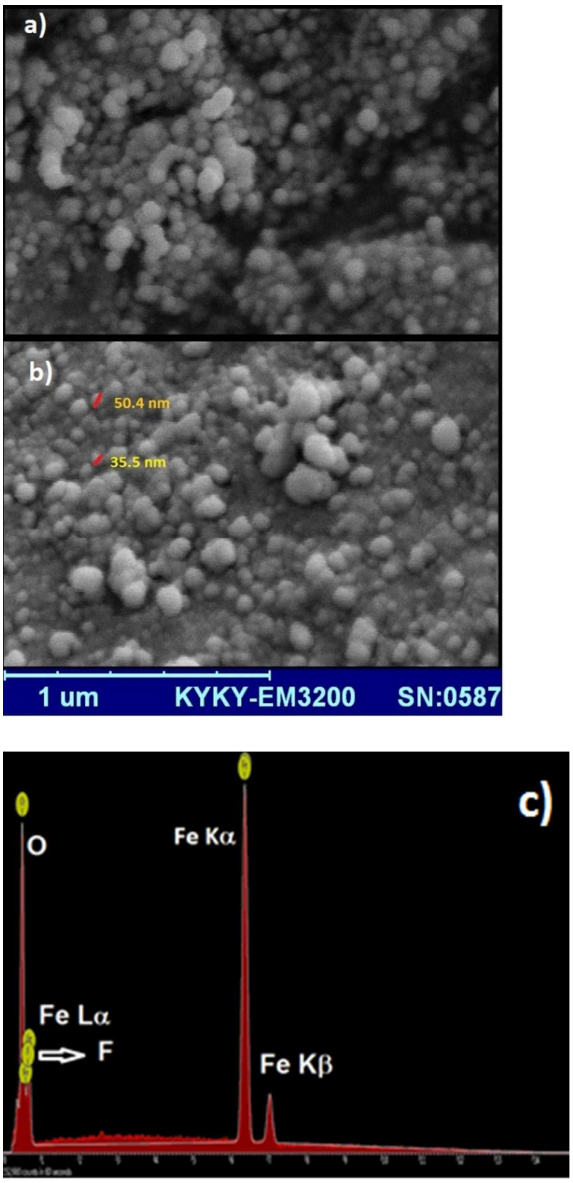

Fig. 1. SEM images of a) MNPs b) BF_3/MNPs-450 and c) EDX Analysis of BF_3/MNPs-450

TEM image of the BF_3/MNPs-450 is shown in Fig. 2. This image demonstrates nearly uniform size of the particles and spherical shape of them.

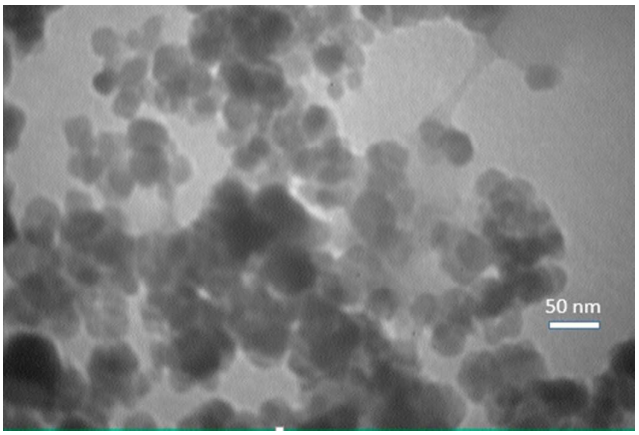

Fig. 2. TEM image of the BF_3/MNPs-450

XRD pattern of magnetite nanoparticles is shown in Fig. 3. Both Fe_3O_4 and BF_3/MNPs-450 show diffraction peaks at 2θ = 30.3, 35.6, 43.3, 53.8, 57.4 and 62.9º that are indexed to the crystalline cubic inverse spinel structure of Fe_3O_4 nanoparticles.

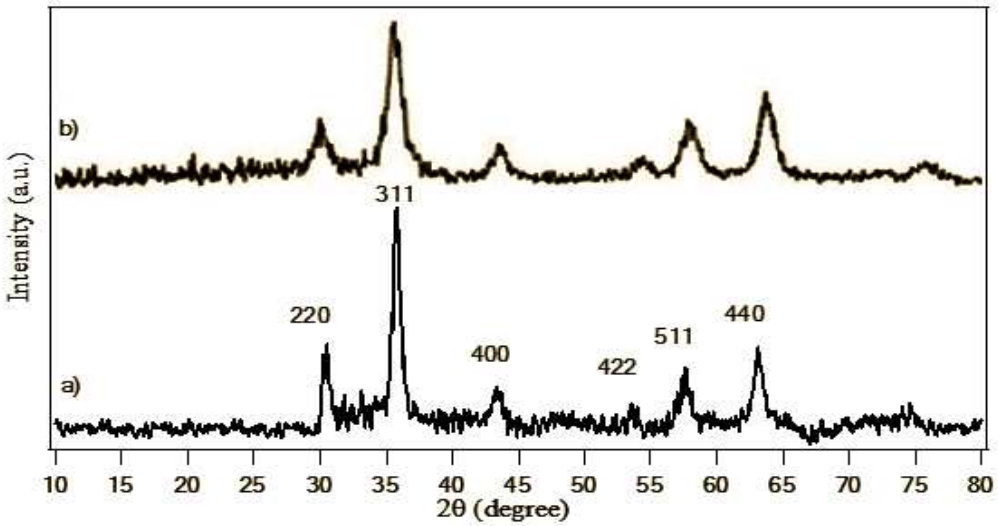

Fig. 3. XRD patterns of a) MNPs and b) BF_3/MNPs-450

Fig. 4 shows the IR spectra of MNPs and BF_3/MNPs at different calcination temperatures over the 400–4000 cm^{-1} region. As shown in Fig. 4, all the samples show characteristic peaks at 560 and 638 cm^{-1}, which are assigned to Fe-O stretching modes. The peak at 1083 is assigned to C-O (the residue of ether) that is not observed in the calcined samples. Apart from the main peaks of MNPs, there is a wide peak at ~1400 cm^{-1}, which is assigned to B–O

stretching [36]. This peak is observed before calcination of the catalyst and also is observed in all calcined samples but with less intensity and partly broadening. Surprisingly, this peak has a larger relative intensity respect to the other calcined samples.

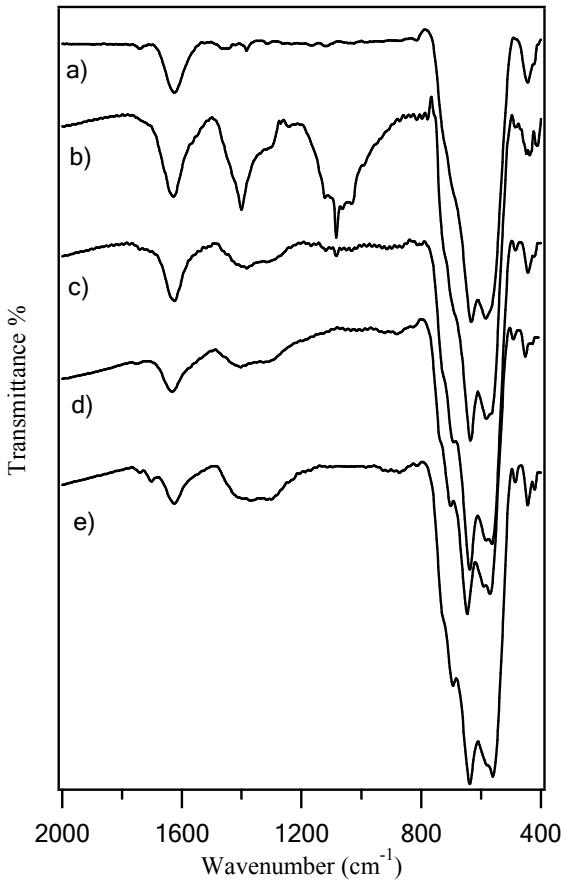

Fig. 4. FT-IR spectra of a) MNPs and BF_3/MNPs b) Before calcination c) calcination at 350 °C d) calcination at 400 °C d) calcination at 450 °C

The catalyst acidity characters, including the acidic strength and the total number of acid sites were determined by potentiometric titration. According to this method, the initial electrode potential (Ei) indicates the maximum acid strength of the surface sites [37]. Therefore, a suspension of the catalyst in acetonitrile was potentiometrically titrated with a solution of 0.02 M *n*-butylamine. As shown in Fig. 5, BF_3/MNPs-450 displays higher strength than the MNPs.

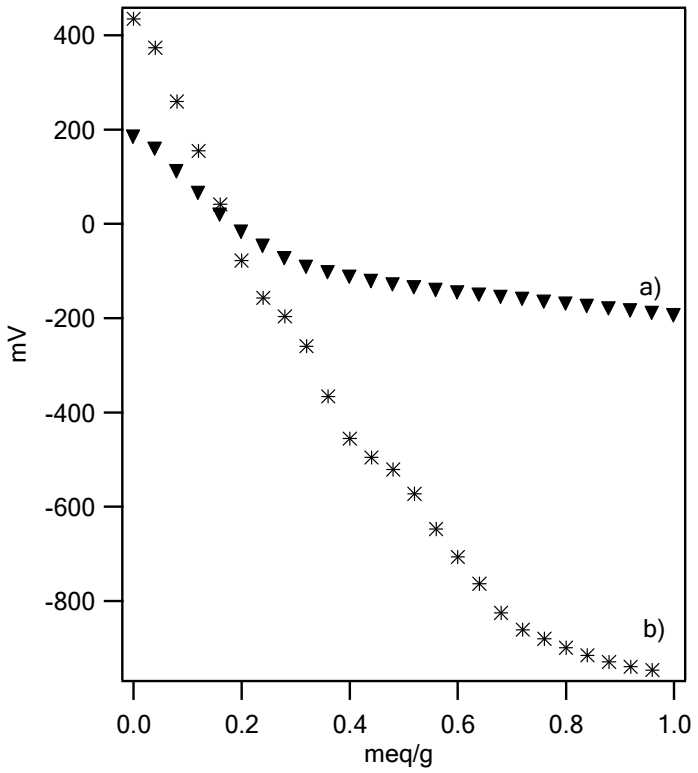

Fig. 5. Potentiometric titration of a) MNPs and b) BF_3/MNPs-450

Fig. 6 shows the magnetization versus applied field of the catalyst that was obtained by VSM. The saturation magnetization value was measured to be ~60 emu g^{-1} for Fe_3O_4 and ~50 emu g^{-1} for BF_3/MNPs-50. The results show that surface modification of MNPs has insignificance effect on the magnetic properties of MNPs.

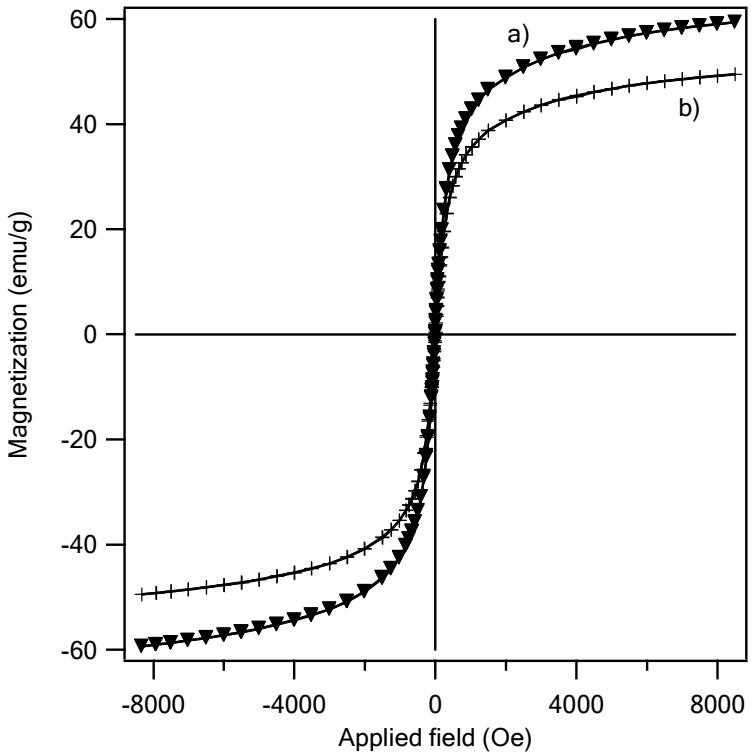

Fig. 6. VSM test of the a) MNPs and b) BF_3/MNPs-450

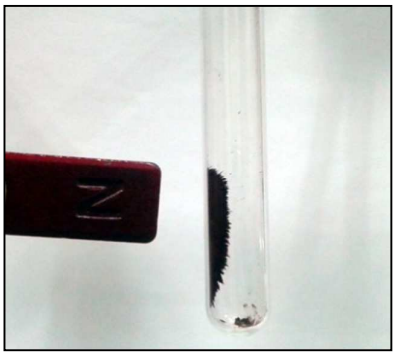

Fig. 7. Representation of catalyst separation with an external magnet

After characterization of the prepared catalysts, to determination of the best catalytic activity, they have been used in the multi-component reaction of 4-chlorobenzaldehyde, malononitrile and 3-methyl-1-phenyl-1H-pyrazol-5(4H)-one as model reaction. The reaction was optimized for various parameters such as temperature, solvent and catalyst loading. We first, investigated effect of the calcination temperature on the catalytic behavior of prepared samples. In the presence of an equal amount of the catalyst (100 mg), BF_3/MNPs-450 show the better catalytic activity in term of the yield of desired product and time of completion of

model reaction in ethanol as the reaction solvent. Therefore, other reaction parameters has been optimized in the presence of BF_3/MNPs-450. To optimize the catalyst amount, the model reaction was performed in the presence of various amounts of the catalyst and according to the obtained results (Table 1, entries 1-4) 100 mg of the catalyst was chosen as the best catalyst amount.

Table 1. Screening of reaction parameters for the synthesis of 1,4-dihydropyrano[2,3-c]pyrazole.

Entry	Catalyst	Catalyst amount (mg)	Time[b] (min)	Yield[c] (%)
1	BF_3/MNPs-450	50	30	86
2	BF_3/MNPs-450	75	20	89
3	BF_3/MNPs-450	100	15	96
4	BF_3/MNPs-450	125	25	79
5	BF_3/MNPs-400	100	60	85
6	BF_3/MNPs-350	100	60	83
7	MNPs	100	180	40
8	$BF_3.Et_2O$	7	35	86

[a]All reactions were carried out with 4-chlorobenzaldehyde (1 mmol), malononitrile (1.1 mmol), 3-methyl-1-phenyl-1H-pyrazol-5(4H)-one (1 mmol), ethanol (5 mL) and BF_3/MNPs-x as the catalyst at 80 °C.

The effect of solvent was also investigated by performing the model reaction in the presence of 100 mg catalyst in various solvents (Table 2, entries 1-5). Among them, ethanol was found to be the best solvent in reflux condition (80 °C) in terms of the reaction time and yield of desired product (Table 2, entry 1). The model reaction in the presence of ethanol as the solvent was also performed at the lower temperature (70 °C) and also the less yield and longer reaction time was obtained (Table 2, entry 6). To investigate efficiency of the support on the catalytic activity of BF_3 the model reaction was performed in the presence of $BF_3.Et_2O$ (7 mg, equal to loading amount of boron on the 100 mg catalyst) and results shows lower activity than BF_3/MNPs-450. MNPs was also applied as the catalyst in the model reaction and results show that MNPs lacks catalytic activity in this type of reaction.

Table 2. Screening of solvents at variable temperature

Entry	Catalyst amount (mg)	Solvent	Temp. (°C)	Time (min)	Yield (%)
1	100	EtOH	80	15	96
2	100	H_2O	100	45	60
3	100	DMF	80	15	90
4	100	THF	65	15	53
5	100	MeOH	65	25	65
6	100	EtOH	70	30	80

[a]All reactions were carried out with 4-chlorobenzaldehyde (1 mmol), malononitrile (1.1 mmol), 3-methyl-1-phenyl-1H-pyrazol-5(4H)-one (1 mmol) and BF_3/MNPs-450 as the catalyst.

Thereafter, the above optimized reaction conditions were explored for the synthesis of 1,4-dihydropyrano[2,3-c]pyrazole derivatives and the results are summarized in Table 3. As exemplified in Table 3, this protocol is rather general for a wide variety of electron-rich as well as electron-deficient aromatic aldehydes.

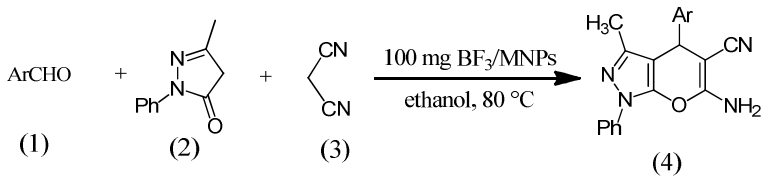

Table 3. BF_3/MNPs-450 catalyzed synthesis of 1,4-dihydropyrano[2,3-c]pyrazole[a]

Entry	Substrate 1	Product 4	Time[b] (min)	Yield[c] (%)	M.p. (°C)[ref]
a	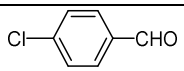	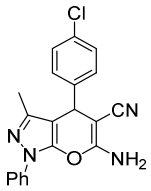	15	96	178-180[38]
b	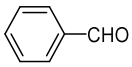	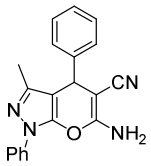	5	88	172-174[38]
c	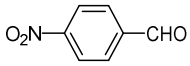	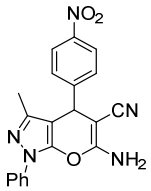	10	90	192-194[38]
d	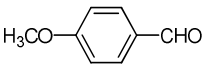	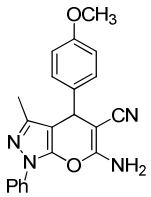	15	85	172-173[38]
e	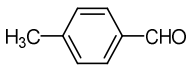	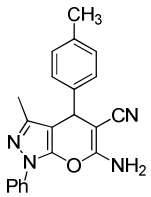	60	93	175-177[38]
f	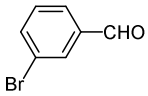	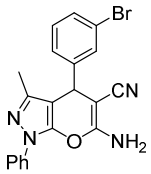	15	87	160-161[39]
g	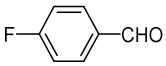	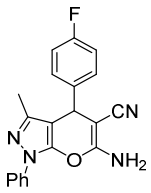	15	84	175-177[40]

h	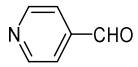	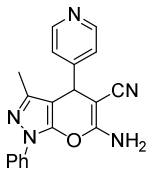	60	90	195-197[27]
i	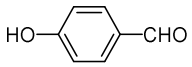	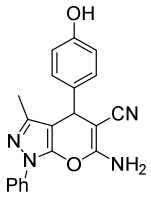	20	88	213-214[38]
j	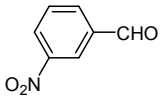	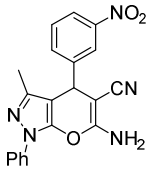	15	91	190-191[40]

[a]All reactions were carried out with 4-chlorobenzaldehyde (1 mmol), malononitrile (1.1 mmol), 3-methyl-1-phenyl-1H-pyrazol-5(4H)-one (1 mmol) in ethanol (5 mL) and BF_3/MNPs-450 as the catalyst at 80 °C.

A Plausible mechanism for the synthesis of pyranopyrazoles catalyzed by BF_3/MNPs is explained in scheme 3.

Scheme 3. Plausible mechanism for the synthesis of pyranopyrazoles catalyzed by BF_3/MNPs

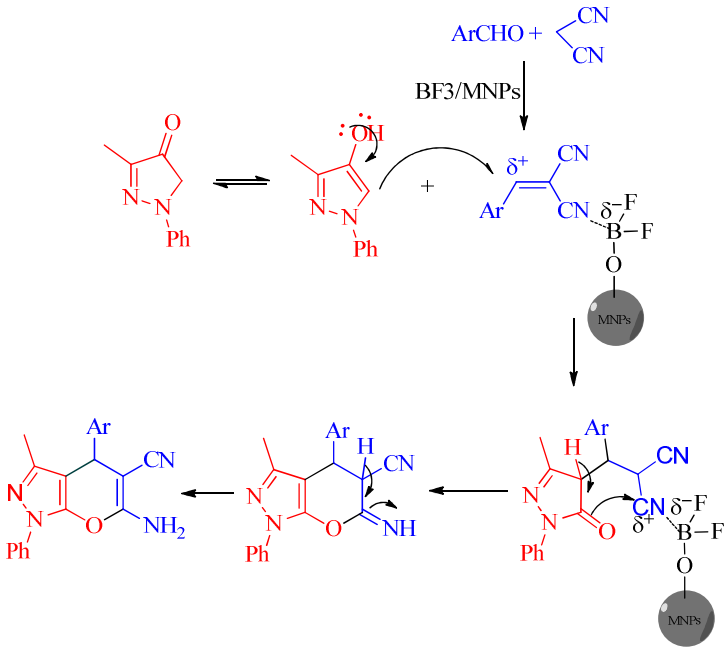

Reusability of the catalyst was investigated in the model reaction under the optimized reaction conditions. The catalyst was separated from the model reaction and reused four times with negligible loss of the catalytic activity (Table 4). Partial loss of activity may be due to blockage of active sites of the catalyst and/or partial leaching of boron from the catalyst.

Table 4. Reusability test of BF_3/MNPs-450 in the model reaction at the optimized conditions

	Fresh catalyst	First cycle	Second cycle	Third cycle	Fourth cycle
Time (min)	15	15	15	15	15
Yield (%)	95	90	88	85	80

A comparative study of this work with other methods has performed. Table 5 presents other reported methods for the synthesis of pyranopyrazole derivatives. Although Table 5 contains various methods such as four-component synthesis of pyranopyrazoles, we can say that our method is comparable with other reported method in terms of yield and reaction time. The most significance of our method is use of the magnetite heterogeneous solid acid catalyst with good catalyst recoverability and ease of separation from reaction media. In addition, use of commercial available precursors, green solvent and easy work-up make this method attractive for the synthesis of pyranopyrazole derivatives.

Table 5. Comparison of this work with other similar works for synthesis of pyranopyrazoles

Entry	Catalyst	Solvent	Temp.(°C)	Time (min)	yields%
1	Uncapped SnO_2 QDs	H_2O	RT	90-150	88-98[41]
2	silica-bonded *N*-propylpiperazine	EtOH	Reflux	15-25	88-95[40]
3	piperidine	H_2O	RT	5-10	67-94[27]
4	BF_3/MNPs	EtOH	Reflux	5-60	84-96[this work]

Conclusion

In conclusion, we prepared BF_3/MNPs as a novel magnetite recoverable catalyst and it has been characterized using various techniques such as SEM, TEM, EDX, XRD, FT-IR and VSM. In this study immobilization of BF_3 on the MNPs was performed through thermal treatment (calcination) and it was observed that calcination temperature have important effect on the catalysis activity of the catalyst. The catalytic activity of the prepared catalysts at the different calcination temperature was investigated in the synthesis of 1,4-dihydropyrano[2,3-c]pyrazole derivatives through one-pot multi-component reaction of aldehyde, malononitrile and 3-methyl-1-phenyl-1H-pyrazol-5(4H)-one and BF_3/MNPs-450 showed better catalytic activity respect to the other samples. From the synthetic method point of view, use of a reusable catalyst, moderate to good yield of products, he simple experimental procedure, easy

workup and ease of the magnetite catalyst recovery make this method attractive for the synthesis of 1,4-dihydropyrano[2,3-c]pyrazole derivatives.

Acknowledgment

We are thankful to the Yazd University Research Council for partial support of this work.

References:

1 T. Vijai Kumar Reddy, G. Sandhya Rani, R. B. N. Prasad and B. L. A. Prabhavathi Devi, *RSC Advances*, 2015, 5, 40997-41005.

2 Y. R. Girish, K. S. Sharath Kumar, U. Muddegowda, N. K. Lokanath, K. S. Rangappa and S. Shashikanth, *RSC Adv.*, 2014, 4, 55800-55806.

3 M. Abdollahi-Alibeik and E. Shabani, *Journal of the Iranian Chemical Society*, 2014, 11, 351-359.

4 H. Tian, X. L. Zhang, J. Scott, C. Ng and R. Amal, *Journal of Materials Chemistry A*, 2014, 2, 6432.

5 N. D. Tran, M. Besson and C. Descorme, *New J. Chem.*, 2011, 35, 2095-2104.

6 S. Fuentes, N. E. Bogdanchikova, G. Diaz, M. Peraaza and G. C. Sandoval, *Catal. Lett.*, 1997, 47, 27-34.

7 M. Hosseini-Sarvari, Z. Razmi and M. M. Doroodmand, *Appl. Catal., A*, 2014, 475, 477-486.

8 M. Abdollahi-Alibeik and A. Moaddeli, *New J. Chem.*, 2015, 39, 2116-2122.

9 M. Abdollahi-Alibeik and A. Moaddeli, *RSC Advances*, 2014, 4, 39759-39766.

10 T. Matsunaga, in *Iron Biominerals*, eds. R. Frankel and R. Blakemore, Springer US, 1991, DOI: 10.1007/978-1-4615-3810-3_6, ch. 6, pp. 79-95.

11 R. K. Singh, T. H. Kim, K. D. Patel, J. C. Knowles and H. W. Kim, *J Biomed Mater Res A*, 2012, 100, 1734-1742.

12 C. Y. Haw, F. Mohamed, C. H. Chia, S. Radiman, S. Zakaria, N. M. Huang and H. N. Lim, *Ceram. Int.*, 2010, 36, 1417-1422.

13 T. Neuberger, B. Schöpf, H. Hofmann, M. Hofmann and B. von Rechenberg, *J. Magn. Magn. Mater.*, 2005, 293, 483-496.

14 S. Ko and J. Jang, *Angew Chem Int Ed Engl*, 2006, 45, 7564-7567.

15 V. Polshettiwar, R. Luque, A. Fihri, H. Zhu, M. Bouhrara and J. M. Basset, *Chem Rev*, 2011, 111, 3036-3075.

16 A. Baiker, H. Baris and R. Schlögl, *J. Catal.*, 1987, 108, 467-479.

17 C. R. F. Lund, J. E. Kubsh and J. A. Dumesic, 1985, 279, 313-338.

18 K. R. P. M. Rao, F. Huggins, V. Mahajan, G. Huffman and V. U. S. Rao, *Hyperfine Interact.*, 1994, 93, 1745-1749.

19 K. Debnath, K. Singha and A. Pramanik, *RSC Advances*, 2015, 5, 31866-31877.

20 A. Khalafi-Nezhad, M. Nourisefat and F. Panahi, *RSC Advances*, 2014, 4, 22497.

21 M. Kotani, T. Koike, K. Yamaguchi and N. Mizuno, *Green Chem.*, 2006, 8, 735.

22 M. B. Gawande, P. S. Branco and R. S. Varma, *Chem. Soc. Rev.*, 2013, 42, 3371-3393.

23 N. J. Thumar, *Arkivoc*, 2010, 2009, 363.

24 P. W. Smith, S. L. Sollis, P. D. Howes, P. C. Cherry, I. D. Starkey, K. N. Cobley, H. Weston, J. Scicinski, A. Merritt, A. Whittington, P. Wyatt, N. Taylor, D. Green, R. Bethell, S. Madar, R. J. Fenton, P. J. Morley, T. Pateman and A. Beresford, *J. Med. Chem.*, 1998, 41, 787-797.

25 J. Skommer, D. Wlodkowic and J. Pelkonen, *Experimental Hematology*, 2006, 34, 463-474.

26 H. V. Chavan, S. B. Babar, R. U. Hoval and B. P. Bandgar, *Bull. Korean Chem. Soc.*, 2011, 32, 3963-3966.

27 G. Vasuki and K. Kumaravel, *Tetrahedron Lett.*, 2008, 49, 5636-5638.

28 M. Babaie and H. Sheibani, *Arabian Journal of Chemistry*, 2011, 4, 159-162.

29 H. Junek and H. Aigner, *Chem. Ber.*, 1973, 106, 914-921.

30 S. Pal, M. N. Khan, S. Karamthulla, S. J. Abbas and L. H. Choudhury, *Tetrahedron Lett.*, 2013, 54, 5434-5440.

31 M. A. Zolfigol, M. Tavasoli, A. R. Moosavi-Zare, P. Moosavi, H. G. Kruger, M. Shiri and V. Khakyzadeh, *RSC Advances*, 2013, 3, 25681.

32 B. Maheshwar Rao, G. N. Reddy, T. V. Reddy, B. L. A. P. Devi, R. B. N. Prasad, J. S. Yadav and B. V. S. Reddy, *Tetrahedron Lett.*, 2013, 54, 2466-2471.

33 Y. Zou, Y. Hu, H. Liu and D. Shi, *ACS Combinatorial Science*, 2012, 14, 38-43.

34 S. H. S. Azzam and M. A. Pasha, *Tetrahedron Lett.*, 2012, 53, 6834-6837.

35 R. Ghosh, L. Pradhan, Y. P. Devi, S. S. Meena, R. Tewari, A. Kumar, S. Sharma, N. S. Gajbhiye, R. K. Vatsa, B. N. Pandey and R. S. Ningthoujam, *J. Mater. Chem.*, 2011, 21, 13388.

36 M. Abdollahi-Alibeik and A. Rezaeipoor-Anari, *Catal. Sci. Technol.*, 2014, 4, 1151-1159.

37 L. R. Pizzio, P. G. Vázquez, C. V. Cáceres and M. N. Blanco, *Appl. Catal., A*, 2003, 256, 125-139.

38 H. S. Sohal, A. Goyal, R. Sharma, R. Khare and S. Kumar, *2013*, 2013, 4.

39 M. Farahi, B. Karami, I. Sedighimehr and H. M. Tanuraghaj, *Chin. Chem. Lett.*, 2014, 25, 1580-1582.

40 K. Niknam, N. Borazjani, R. Rashidian and A. Jamali, *Chinese. j. catal.*, 2013, 34, 2245-2254.

41 S. Paul, K. Pradhan, S. Ghosh, S. K. De and A. R. Das, *Tetrahedron*, 2014, 70, 6088-6099.